

# Temporal Dynamics of Greenhouse Gas Flux of Warm Temperate Deciduous Broad-Leaved Forest Ecosystem Soil in North China

Wuxing Wan (✉ [wan.wx1972@126.com](mailto:wan.wx1972@126.com))

Hebei Normal University <https://orcid.org/0000-0002-6106-517X>

Shuai Zhang

Hebei Normal University

Jie Li

Hebei Normal University

Yiqin Gao

Hebei Normal University

Meiqi Feng

Hebei Normal University

Xiaohe Wang

RCEES: Research Centre for Eco-Environmental Sciences Chinese Academy of Sciences

---

## Research

**Keywords:** Greenhouse Gas Flux, Warm Temperate Deciduous Broad-Leaved Forest Ecosystem, North China

**Posted Date:** May 4th, 2021

**DOI:** <https://doi.org/10.21203/rs.3.rs-455687/v1>

**License:** © ⓘ This work is licensed under a Creative Commons Attribution 4.0 International License.

[Read Full License](#)

---

1 Temporal Dynamics of Greenhouse Gas Flux of Warm Temperate  
2 Deciduous Broad-Leaved Forest Ecosystem Soil in North China

3 Wuxing Wan<sup>1\*</sup>, Shuai Zhang<sup>1</sup>, Jie Li<sup>1</sup>, Yiqin Gao<sup>1</sup>, Meiqi Feng<sup>1</sup> and  
4 Xiaoke Wang<sup>2\*</sup>

5 **Abstract**

6 **Background:** According to the WMO's (World Meteorological Organization)  
7 Greenhouse Gas Bulletin (2019), the fastest increase atmospheric concentrations of the  
8 three main greenhouse gases has been detected in the past 20 years. Researchers have  
9 paid more and more attention to the problem of greenhouse gas (GHG) emission.  
10 Among the studies, people focus much more on grassland ecosystem than that of forest  
11 ecosystem, which has a more important effect on the emission and absorption of  
12 greenhouse gases. Estimating the impact of forest ecosystem on greenhouse effect in  
13 China is of great significance.

14 **Methods:** 6 deciduous broad-leaved forest communities with similar elevation, slope  
15 orientations and slope gradient in Wuling Mountain National Natural Reserve are  
16 employed to conduct the GHG flux study. Five 50cm×50cm square stainless-steel bases  
17 are set in the study site by mechanical spot arrangement method to sample the GHG.  
18 The environmental temperature and soil moisture content is measured every sampling  
19 time. Static chamber-gas chromatograph method is adopted to examine the greenhouse  
20 gas fluxes of CO<sub>2</sub>, CH<sub>4</sub> and N<sub>2</sub>O.

21 **Results and conclusions:** The GHG flux of CO<sub>2</sub>, N<sub>2</sub>O and CH<sub>4</sub> in the Warm Temperate  
22 Deciduous Broad-Leaved Forest Ecosystem has great relationship with environmental  
23 temperature and soil water content. GHG flux varies with seasons. Among them, the  
24 CH<sub>4</sub> flux shows the character of source or sink in different seasons. The other 2 are  
25 always the source of GHG flux during the study period. The peak value of CO<sub>2</sub> is in  
26 summer and that of N<sub>2</sub>O in March. The flux of CH<sub>4</sub> shows the feature of source in April  
27 and sink in other seasons. The peak value of sink comes in late July. The flux of CO<sub>2</sub>  
28 has the greatest relationship with the soil temperature 5cm below the ground surface  
29 and the flux of N<sub>2</sub>O has the greatest relationship with the soil water content. The  
30 relationship between CH<sub>4</sub> flux and the environmental temperature or the soil water  
31 content is complex.

32 **Key words:** Greenhouse Gas Flux, Warm Temperate Deciduous Broad-Leaved Forest  
33 Ecosystem, North China

34

## 35 **Background**

36 With the development of global industrialization, greenhouse Gases (GHG) in the  
37 atmosphere caused by human activities have increased significantly. There are kinds of  
38 gases that can leads to the Greenhouse Effect, among which the three gases that  
39 contribute the most to the greenhouse effect include CO<sub>2</sub>, N<sub>2</sub>O and CH<sub>4</sub>.

40 CO<sub>2</sub> is the most important greenhouse gas except water vapor (IPCC 2000). The  
41 100-year Global Warming Potential (GWP) of N<sub>2</sub>O is 310 times that of CO<sub>2</sub>, which  
42 makes its contribution to the greenhouse effect approximately 6% (Bouwman et al.  
43 2002; IPCC 1996). The GWP of CH<sub>4</sub> is about 25 times that of CO<sub>2</sub> (Hansen et al. 1990).  
44 Almost one third of global CH<sub>4</sub> emissions come from natural sources (Bras et al. 2001),  
45 and although its growth rate is lower than that of CO<sub>2</sub>, it contributes about 20% to the  
46 greenhouse effect caused by greenhouse gases (Sims et al. 2014).

47 According to the WMO's (World Meteorological Organization) Greenhouse Gas  
48 Bulletin (2019), the fastest increase atmospheric concentrations of the three main  
49 greenhouse gases has been detected in the past 20 years. The power for the increase of  
50 GHG content in atmosphere can be divided into 2 categories: one is the vast use of  
51 fossil fuels; the other includes some natural process effects and land-use change (WMO,  
52 2009). Due to the increase of greenhouse gas content in the atmosphere, which  
53 exacerbates global climate change, researchers have paid more and more attention to  
54 the problem of GHG emission (Apps et al. 1993; Song Changchun et al. 2006; Zhang  
55 Lihua, 2005; Nikunja et al. 2018; Marissa et al. 2019).

56 Forest is the largest carbon pool in terrestrial ecosystems (Sedjo, 1993). It has the  
57 widest distribution area, highest productivity and largest biomass accumulation  
58 compared to other vegetation types. Any increase or decrease of forest ecosystem  
59 carbon storage will affect the atmospheric CO<sub>2</sub> concentration. The carbon cycle process  
60 of forest ecosystem regulates the dynamics of global terrestrial carbon cycle (Li et al.  
61 2003). Among the studies reported on the global estimation of carbon storage and flow,  
62 people focus much more on grassland ecosystem than that of forest ecosystem. Forests  
63 account for 23.04% of the land area in China (2021) (<http://www.forestry.gov.cn/>). It  
64 has an important effect on the emission and absorption of greenhouse gases. Estimating  
65 the impact of forest ecosystem on greenhouse effect in China is of great theoretical and  
66 practical significance for exerting forest ecological benefits effectively and alleviating  
67 global warming. In this research, the characteristics of greenhouse gas flux in warm  
68 temperate deciduous broad-leaved forest ecosystem are studied by static chamber-gas

69 chromatograph method.

70

## 71 **Methods and materials**

### 72 **Plots setting**

73 49 deciduous broad-leaved standard forest plots with 400 m<sup>2</sup> horizontal area has  
74 been set in the Wuling Mountain National Reserve in 2011. To make sure that the study  
75 results have scientific comparability among the sample plots, 6 deciduous broad-leaved  
76 forest communities with similar elevation, slope orientations and slope gradient are  
77 employed to conduct the GHG emission study. The 6 chosen plots are all set on the  
78 shady slope between 26° and 30° gradient at about 1000 m elevation. Since March 2013,  
79 gas samples are collected every three weeks.

### 80 **Sampling with static chamber**

81 Static chamber-gas chromatograph method is adopted to monitor the greenhouse  
82 gas fluxes of CO<sub>2</sub>, CH<sub>4</sub> and N<sub>2</sub>O. Five 50cm×50cm square stainless-steel bases are set  
83 in the study site by mechanical spot arrangement method. The upper surface of the base  
84 is kept horizontal for water sealing. The static chamber is made with transparent acrylic  
85 plate. Tube with an inner diameter of 2mm and a length of 1.5m is used to balance the  
86 air pressure inside and outside the static chamber. Digital thermometers and mercurial  
87 thermometers are employed to measure the environment temperatures. The water  
88 content of the soil is measured. The soil surface temperature is measured by the Smart  
89 Sensor AR320 infrared thermometer. JM222U portable digital surface thermometer is  
90 used to measure the air temperature and the temperature in the static chamber. Using  
91 mercury thermometer to measure soil temperature of 5cm beneath the surface. The 0-  
92 20 cm topsoil near the static chamber is sampled with a soil drill. Collected gas samples  
93 is analyzed by Agilent 7890A gas chromatograph within 72h.

### 94 **Monitoring implementation**

95 Gas samples are collected every 3 weeks from March to November in 2013. To  
96 make sure that the environment temperature is as close to the daily average as possible,  
97 sampling begins at 10:00 am every time. The first sample are collected when the  
98 chamber is set simultaneously, and then samples would be collected once every 10min.  
99 During a period of 30min, a total of 4 gas samples are collected. Samples are collected  
100 in 500ml aluminum - plastic composite air bags. The ambient air temperature, the  
101 temperature in the tank and the soil temperature of 5cm below the surface are measured

102 simultaneously in situ. The 0 - 20 cm surface soil are sampled to measure the soil  
103 moisture content.

#### 104 **Analyzing for GHG flux**

105 Flux refers to the physical quantity transported through a unit area interface per  
106 unit time. The concentration of the test sample is calculated as follow:

$$107 \quad C_s = A_s \times C_0 \div A_0$$

108  $C_s$ : Test sample concentration;  $C_0$ : concentration of standard gas;  $A_s$ : peak area of  
109 test sample;  $A_0$ : area of standard gas peak.

110 Greenhouse gas flux is calculated by the following formula:

$$111 \quad F = \frac{\rho \cdot V \cdot \Delta C}{A \cdot \Delta t}$$

112 Where:  $F$  is the flux of measuring gas,  $\rho$  is the density of monitoring gas,  $\Delta C$  is  
113 the variation in the concentration of monitoring gas,  $\Delta t$  is the length of monitoring time,  
114  $A$  and  $V$  are the area at the bottom of the sampling box and the volume of the gas  
115 chamber respectively. When the value of  $F$  is negative, it indicates that the soil absorbs  
116 the greenhouse gas, showing the flux characteristics of "sink". When the value of  $F$  is  
117 positive, it indicates that the soil emits the greenhouse gas, showing the flux  
118 characteristics of "source".

119 Statistical analysis of data is performed by Excel (16) and SPSS 22.

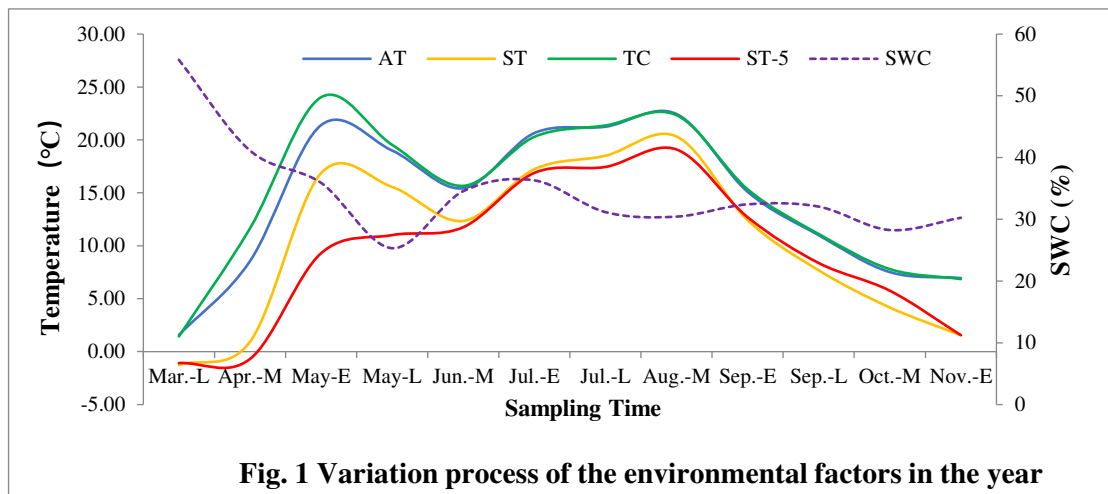
## 120 **Results and Analysis**

### 121 **Dynamics of environmental factors in different seasons**

122 The dynamic process of environmental factors including environmental  
123 temperatures and soil water content for the sampling plots in a year are analyzed. (Fig.  
124 1). It can be seen from Fig. 1 that the soil moisture content reached the peak of the year  
125 in the first monitoring in March 2013. The average moisture content of the 6 study  
126 sample plots is close to 60%. This result should be related to the heavy snow in the  
127 winter of 2012. But the soil is still in the frozen state. The average soil temperature 20  
128 cm below the surface is about  $-2^{\circ}\text{C}$  -  $-3^{\circ}\text{C}$ . Soil water cannot exert influence effectively  
129 on the ecological process happened in the soil. In the subsequent process, the water  
130 content is in the process of decreasing until late May. This is mainly because that the  
131 study area is still in the dry season with very little precipitation during this period.  
132 However, with the rise of temperature and the absence of leaves for the canopy, the

133 ground of the ecosystem is completely open for evaporation from the soil water. As a  
 134 result, the surface soil can be heated up rapidly and the evapotranspiration intensified.  
 135 And then, the soil moisture content is in the process of decreasing from March to the  
 136 end of May.

137 Environmental factors are: AT: air temperature; ST: surface temperature of the soil; TC: temperature  
 138 in the chamber; ST-5: soil temperature of 5cm below the surface; SWC: soil water content  
 139 Monitoring time includes: Mar.-L: 3.27-4.1; Apr.-M: 4.13-4.18; May-E: 5.4-5.9; May-L: 5.22-5.27;  
 140 Jun.-M: 6.8-6.13; Jul.-E: 6.30-7.4; Jul.-L: 7.18-7.23; Aug.-M: 8.11-8.16; Sep.-E: 9.2-9.7; Sep.-L:  
 141 9.23-9.28; Oct.-M: 10.11-10.16; Nov.-E: 11.3-11.8.  
 142 And: E for early, M for middle, L for late.



143  
 144 It gradually enters the rainy season from June in the Wuling Mountain National  
 145 Reserve. The precipitation increases and the soil water is replenished. From June to  
 146 October 2013, the soil water content for the monitoring plots is in a relatively stable  
 147 state. Precipitation in this region is concentrated in June to July and September of 2013,  
 148 so the soil water content showed two small peaks in the corresponding period.

149 From the point of dynamic process of the environmental temperature in the year,  
 150 the average temperature for the 6 plots of the diverse temperature indicators always  
 151 presents the characteristics that temperature inside the chamber > air temperature >  
 152 surface temperature > soil 5cm temperature. Due to the rapid increase of ambient  
 153 temperature and the opening of the canopy of the ecosystem, the temperature indices  
 154 reached their maximum value in May. With the closure of the arbor layer and the  
 155 beginning of the rainy season, the ambient temperature is getting lower in June. But it  
 156 reached its peak value again in the middle of August, the hottest days in the summer,  
 157 which is similar to that in the middle of May.

158 The warm temperate zone in the continental monsoon climate region is roughly

159 between 32° – 43° N. Wuling Mountain National Nature Reserve is located at 40°29' –  
160 40°38', which belongs to the high latitude area of warm temperate zone. In addition, the  
161 altitude of the study sites is relatively high (the average altitude of the 6 plots is about  
162 1 000 m). It has been in the process of cooling since August. By November, the soil  
163 surface temperature is close to 0°C, reaching the lowest level in this monitoring stage.  
164 The temperature in the static chamber is always a little bit higher than the ambient  
165 temperature due to the combined effect of illumination, sealing and soil respiration. The  
166 temperature in the chamber, the air temperature and the surface temperature are in a  
167 similar dynamic process for the whole year (Fig. 1).

168 Due to the covering effect of the litters over the ground, soil temperature 5 cm  
169 below the surface rise slower than other temperature indices. It didn't climb the peak  
170 consistent with the air temperature in May. Whereas, under the combined influence of  
171 factors such as air temperature, precipitation, soil temperature 5 cm below the surface  
172 shew a long durable plateau from early May to middle June, raised from late June and  
173 peaked in August. Then, it continued to reduce together with the dropping of the air  
174 temperature.

175 Taking the environmental temperature and soil moisture into account  
176 comprehensively, they entered a rapid changing process from the beginning of  
177 environmental warming and soil freeze-thaw in spring. From June to August, summer  
178 and rainy season are in this region. After entering this stage, environmental temperature  
179 and soil hydrology are in a stable and slowly rising period. The air temperature is the  
180 highest in August, and rainfall is also the most concentrated simultaneously. After  
181 September, the environmental temperature and soil moisture continued to decrease in  
182 the relatively dry autumn and winter in this region.

## 183 **Temporal variation characteristics of greenhouse gas flux**

### 184 **1. Diurnal dynamic process**

185 Due to the variation of solar radiation intensity and the air temperature in the  
186 daytime from morning to night, as the main influencing factors to the greenhouse gas  
187 flux, the soil temperature and soil moisture varies with the time through the day. The  
188 activity of the roots of the plants, soil microbials and soil animals will fluctuate with  
189 time. The rate of greenhouse gas emissions or deposit will be diverse in different time.  
190 The variation process of greenhouse gas flux from morning to night is monitored per  
191 hour on April, July and September respectively. The result is employed to estimate the  
192 greenhouse gas flux in warm temperate deciduous broad-leaved forest ecosystems (Fig.

193 2).

194

### 195 (1) Process of CO<sub>2</sub> flux

196 The results show that CO<sub>2</sub> is the source of greenhouse gas flux in warm temperate  
197 deciduous broad-leaved forests in all seasons. In the hourly diurnal variation monitoring,  
198 the emission level in July is the highest, while that in April is the lowest, indicating that

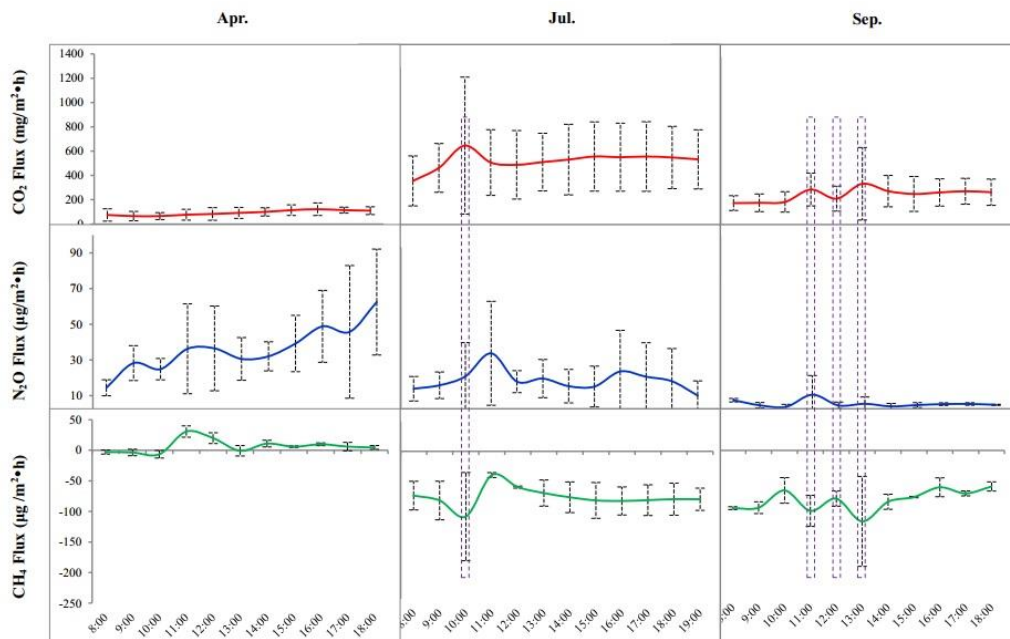


Fig. 2 Dynamic process of GHGs flux rate during a day in different seasons

199 the emission level of CO<sub>2</sub> in summer is higher than that in other seasons. Basing on the  
200 process of diurnal variation, the flux of CO<sub>2</sub> in April has been rising steadily at a low  
201 level from 8 o'clock in the morning, reaching the peak at 16 o'clock in the  
202 afternoon and then decreased. In July, the peak value reached at 10 o'clock and had no  
203 significant change until 19 o'clock. In September, there are two peaks at 11 o'clock and  
204 13 o'clock. Basing on the monitored CO<sub>2</sub> diurnal emission process in three seasons, the  
205 daytime CO<sub>2</sub> emission showed a tendency of continuous increase on the whole.

### 206 (2) Process of N<sub>2</sub>O flux

207 The flux process in a year of N<sub>2</sub>O are different from that of CO<sub>2</sub>, with the highest  
208 emission level occurring in April rather than July in summer. In the research plots, April  
209 is the soil freeze-thaw season. Studies have shown that a large amount of N<sub>2</sub>O is  
210 discharged from the soil in the period of soil freeze-thaw (Li et al. 1999). In April, the  
211 diurnal flux variation showed that the emission level is high and continued to rise during  
212 the day from morning to night. The diurnal variation pattern of July is different from

213 that of April. In this season, the total daytime emission level is relatively stable, but  
214 there are two peaks at 11 o'clock and 16 o'clock. N<sub>2</sub>O emissions in September are  
215 significantly lower than in April and July. Diurnal flux is stabilizing at lower level  
216 except for a peak at 11 o'clock.

### 217 **(3) Process of CH<sub>4</sub> flux**

218 The diurnal variation of CH<sub>4</sub> flux is relatively complex. The monitoring results  
219 show that the diurnal CH<sub>4</sub> flux in April generally presents the characteristics of source,  
220 with an obvious peak at 11 o'clock and another lower peak at 14 o'clock. The flux at  
221 the rest of the monitoring time is relatively stable. And in July and September, it  
222 performed as a sink. From the diurnal variation characteristics of sink, the peak for CH<sub>4</sub>  
223 absorption appeared simultaneously with the peak for CO<sub>2</sub> emission. It indicates that  
224 there could be a direct relationship between CH<sub>4</sub> and CO<sub>2</sub> in the process of source-sink  
225 flux.

## 226 **2. Seasonal dynamics of GHG**

### 227 **(1) CO<sub>2</sub> flux in different seasons**

228 According to the diurnal process and seasonal variations of CO<sub>2</sub> flux, the dynamic  
229 processes in different seasons of the 6 plots are estimated (Fig. 3). The results show that  
230 the CO<sub>2</sub> emission process in a year presents a single peak curve in general and reached  
231 its peak in mid-August. There are differences in CO<sub>2</sub> flux among different plots. The  
232 total emission level of plot 1 and plot 6 is higher, while plot 4 is the lowest. Many  
233 studies have shown that the CO<sub>2</sub> flux has the highest emission rate in summer, followed  
234 by that in spring and autumn, and the lowest emission rate in winter (Wang et al. 2004),  
235 which is consistent with the conclusion of this study.

236 The characteristic of the CO<sub>2</sub> flux dynamic is mainly caused by seasonal changes  
237 in temperature and soil moisture content. In summer, higher soil temperature and water  
238 content enhance microbial activity and root respiration. Total soil respiration is  
239 promoted (Li et al. 1987). The CO<sub>2</sub> emission rate in rainy season is much higher than  
240 that in dry season (Chen et al. 2004). There has been another study on the greenhouse  
241 gas emission flux and dynamics of forest soil in the West Mountain area of Beijing (Sun  
242 et al. 1999). The result show that when the soil temperature in winter is below zero,  
243 forest soil acted as a sink for CO<sub>2</sub>. Whereas, our study did not find that the same result  
244 of a sink for CO<sub>2</sub> in winter, which is different from the research conducted in West  
245 Mountain of Beijing. The two study regions belong to a similar climatic zone and the  
246 difference in latitude between the two places is about 0.6° only. More study is needed

247 to uncover the reason for the different characteristics of CO<sub>2</sub> flux in winter between the  
248 2 places.

249

## 250 (2) N<sub>2</sub>O flux in in different seasons

251 The dynamic process of N<sub>2</sub>O flux in a year is different from that of CO<sub>2</sub>, which  
252 shows high emissions in 5 of the 6 plots at the end of March (Fig. 4). The remaining  
253 one of plot 1 claimed its N<sub>2</sub>O emission peak in April. Two other small peaks occurred

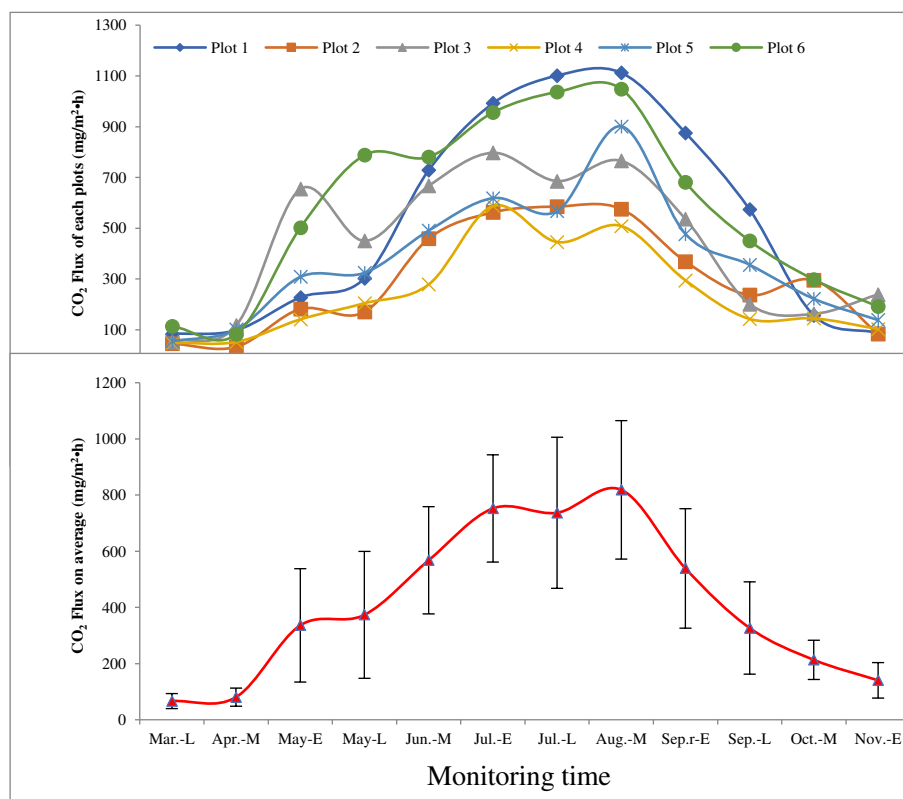


Fig. 3 Dynamic process of CO<sub>2</sub> flux rate in different seasons

254 in early July and mid-August. According to the average emission level of the 6 plots  
255 overall, the N<sub>2</sub>O emission level is the highest in late March at an average emission rate  
256 close to 100  $\mu\text{g}/\text{m}^2\cdot\text{h}$ . The peak in mid-July is close to 50  $\mu\text{g}/\text{m}^2\cdot\text{h}$ , and the other small  
257 peak appeared in mid-August is close to 20  $\mu\text{g}/\text{m}^2\cdot\text{h}$ .

258 The production process of soil N<sub>2</sub>O is very complex and is affected by many  
259 environmental factors (Li et al. 1999), among which the soil temperature, soil water  
260 content and precipitation before sampling have the most significant effects on the  
261 monitoring result of soil N<sub>2</sub>O flux. In addition, the difference of soil C and N content  
262 and various environmental factors that have an effect on metabolic processes such as  
263 respiration, nitrification and denitrification all have an impact on soil N<sub>2</sub>O flux.

264 Therefore, the characteristics of N<sub>2</sub>O flux have significant spatial and temporal  
265 specificity.

266

267 Some studies have shown that N<sub>2</sub>O emissions are the highest in summer, followed  
268 by spring and autumn, and the lowest or even negative in winter (Sun et al. 2001; Teepe  
269 et al. 2004). In this study, the peak of soil N<sub>2</sub>O emission in the warm temperate  
270 deciduous broad-leaved forest occurs in April, which is different from the research

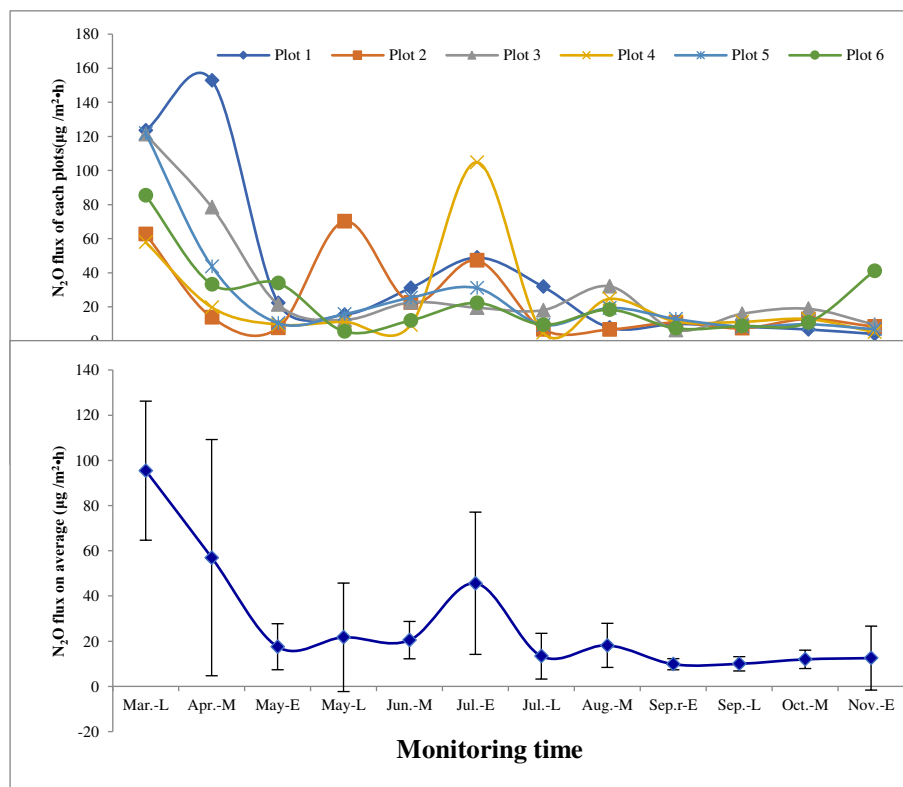


Fig. 4 Dynamic process of N<sub>2</sub>O flux rate in different seasons

271 results of Sun Xiangyang (2001) and Teepe (2004). The reasons for the difference  
272 among the studies need further revealing.

### 273 (3) CH<sub>4</sub> flux in in different seasons

274 It is found that CH<sub>4</sub> flux in the warm temperate deciduous broad-leaved forest  
275 ecosystem had seasonal variation between source and sink. The CH<sub>4</sub> flux for 5 of the 6  
276 monitoring plots, except plot 2, showed the characteristics of source in mid-April. The  
277 overall average level of CH<sub>4</sub> flux on this time of each ecosystem also showed the  
278 characteristics of source (Fig. 5). In other monitoring periods in the year, the soil of the

279 warm temperate deciduous broad-leaved forest ecosystem showed CH<sub>4</sub> sinks.

280

281 On the average CH<sub>4</sub> flux level of the 6 study plots in a year, as a function of sink,

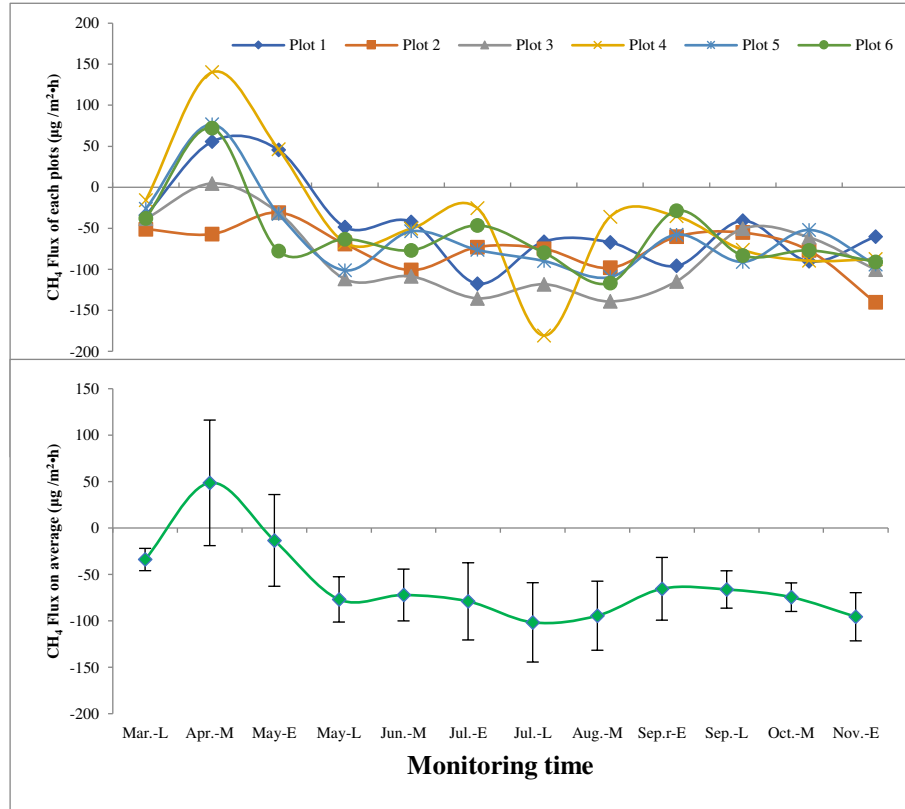


Fig. 5 Dynamic process of CH<sub>4</sub> flux rate in different seasons

282 the highest CH<sub>4</sub> absorption of forest soil occurred from late July to mid-August. Soil  
283 temperature, soil moisture content, soil physical and chemical properties and changes  
284 in land use patterns will affect the characteristics of soil CH<sub>4</sub> flux (Li et al. 1999).

## 285 Conclusions

286 1) Soil moisture reached its peak in March 2013 and showed a downward trend  
287 until the end of May. After June, it entered the rainy season, and the soil moisture  
288 stabilized at about 30%. The ambient temperature always presents the relationship that:  
289 temperature inside the chamber > air temperature > surface temperature > soil  
290 temperature 5cm below the surface. Ambient temperature has two peaks in May and  
291 August. Since August, it has been in the process of cooling, and by November, the  
292 surface temperature has been close to 0°C.

293 2) There were significant seasonal differences in the diurnal variation of GHG  
294 fluxes. The maximum value of CO<sub>2</sub> was in summer, and the peak value of daily flux  
295 appeared at 10:00 am. It's flux level in autumn was lower than that in summer, and two

296 peaks appeared at 11:00 and 13:00. The emission level of N<sub>2</sub>O was the highest and rose  
297 in April. Then the emission level of N<sub>2</sub>O was higher in summer than in autumn. The  
298 peak value in summer was at 11:00 and 16:00, and the peak value in autumn was at  
299 11:00 in the morning. In April, CH<sub>4</sub> flux shows the characteristics of source overall. In  
300 summer and autumn, then is a sink. And the peak of sink occurs at the same time as  
301 CO<sub>2</sub>.

302 3) The seasonal dynamic process of CO<sub>2</sub> flux is a unimodal curve and the peak is  
303 in summer. The N<sub>2</sub>O flux peaked in March, and then two peaks appeared in early July  
304 and mid-August, and the peak value in July was higher than that in August. CH<sub>4</sub> flux  
305 showed as a source in April and a sink in other seasons. The peak of absorption appeared  
306 in late July.

307 4) The seasonal dynamic of CO<sub>2</sub> flux is consistent with the ambient temperature,  
308 especially the soil temperature 5cm below the surface. The seasonal dynamic of N<sub>2</sub>O  
309 flux is consistent with the topsoil water content, and the source-sink capacity of CH<sub>4</sub>  
310 flux is opposite to the soil moisture content. The dynamic relationship between CH<sub>4</sub>  
311 and N<sub>2</sub>O fluxes and temperature is complex.

312

### 313 **Acknowledgements**

314 We thank the support of Wuling Mountain National Nature Reserve Administration.  
315 Traffic problem smoothly resolved. The filed study could not be conducted without the  
316 help from Dongyi Li, Xuequan Feng, Jianguo Sun, Yafei Xiang, Jian'gang Guo and  
317 Zhifu Wu.

### 318 **Authors' contributions**

319 Wuxing wan designed the study and developed the whole process, including all the  
320 sampling work, data monitoring and analysis of the result. Xiaoke Wang provided  
321 comprehensive guidance to the design, implementation and data analysis of the study.  
322 Shuai Zhang and Jie Li collected and prepared the data. Yiqin Gao and Meiqi Feng  
323 analyzed the data and draw the diagram. All authors contributed and approved the final  
324 manuscript.

### 325 **Funding**

326 We acknowledge funding by Science and Technology Project of Hebei Education  
327 Department (ZD2015091) and project of Natural Science Foundation of Hebei Province  
328 (C2017205152).

### 329 **Availability of data and materials**

330 The datasets used and/or analyzed during the current study are available from the

331 corresponding author on reasonable request.

### 332 **Declarations**

333 Ethics approval and consent to participate

334 Not applicable.

335 Consent for publication

336 Not applicable.

337 Competing interests

338 The authors declare that they have no competing interests.

### 339 **Author details**

340 <sup>1</sup>College of Life Sciences, Hebei Normal University, Shijiazhuang 050024, China

341 <sup>2</sup>State Key Laboratory of Urban and Regional Ecology, Research Center for Eco-

342 Environmental Sciences, Chinese Academy of Sciences, Beijing 100085, China

343

### 344 **References**

345 Apps M. J., Kurz W.A., Luxmoore R.J. Boreal forests and tundra [J]. *Water, Air, and Soil Pollution*,  
346 1993,70(1-4):39-53.

347 Bouwman A. F., Boumans L. J. M., Batjes N. H. Emissions of N<sub>2</sub>O and NO from fertilized fields:  
348 Summary of available measurement data [J]. *Global Biogeochemical Cycles*, 2002,16(4):6-1-  
349 6-13.

350 Bras O., Guillou C., Reniero F. The global methane cycle: isotope and mixing ratios, sources and  
351 sinks[J]. *Isotopes in environmental and health studies*, 2001,37(4):257-379.

352 Chen P. Q. *Carbon Cycle in Earth System* [M]. China Science Press, Beijing, 2004:266-268.

353 Hansen J, Fung I, Lacis A, et al. Global climate changes as forecast by Goddard Institute for Space  
354 Studies three-dimensional model[J]. *Journal of Geophysical Research: Atmospheres* (1984-  
355 2012), 1988,93(D8):9341-9364.

356 International Panel on Climate Change, Working Group 1 Third Assessment Report. Cambridge  
357 Univ. Press, Cambridge, MA, 2001.

358 IPCC. *The Revised 1996 IPCC Guidelines for National Greenhouse Gas Inventories, Reference*  
359 *Manual*. UK Meteorological Office, Bracknell, 1997.

360 Li G, Jiang R, Fu Y. Phytomass and the seasonal dynamics of an alpine meadow in  
361 Tianzhu[C]//*Proceedings of the International Symposium on Grassland Vegetation*. Hohhot,  
362 PR China. 1987:407-412.

363 Li Haitao, Shen Wenqing, Liu Qijing, Yu Guirui. On the Study of Carbon Cycle in Wetland  
364 Ecosystems[J]. *Jiangxi Science*, 2003,21(3):160-167.

365 Li Yu 'e, Lin Erda. Progress in Study on Methane Uptake by Aerobic Soil[J]. Advance in Earth  
366 Sciences. 1999,14(6):613-618.

367 Marissa Malahayati, Toshihiko Masui. The impact of greenhouse gas mitigation policy for land use  
368 and the forestry sector in Indonesia: Applying the computable general equilibrium model[J].  
369 Forest Policy and Economics, 2019,(109), 102003.

370 Nikunja Mohan Modak a, Debabrata Kumar Ghosh b, Shibaji Panda c, Shib Sankar Sana d.  
371 Managing greenhouse gas emission cost and pricing policies in a two-echelon supply chain.  
372 CIRP Journal of Manufacturing Science and Technology, 2018,(20):1-11.

373 Sedjo R A. The carbon cycle and global forest ecosystem[J]. Water, Air, and Soil Pollution,  
374 1993,70(1-4):295-307.

375 Sims R, Schaeffer R, Creutzig F, et al. Transport. In: Climate Change 2014: Mitigation of Climate  
376 Change. Contribution of Working Group III to the Fifth Assessment Report of the  
377 Intergovernmental Panel on Climate Change[M]. 2014.

378 SONG Chang-chun, ZHANG Li-hua, WANG Yi-yong, ZHAO Zhi-chun. Annual Dynamics of CO<sub>2</sub>,  
379 CH<sub>4</sub>, N<sub>2</sub>O Emissions from Freshwater Marshes and Affected by Nitrogen Fertilization[J].  
380 Environmental Science, 2006,27(12):2369-2375.

381 Sun xiangyang, Xu huacheng. Emission flux of nitrous oxide from forest soil in Beijing[J]. Scientia  
382 Silvae Sinicae. 2001,37(5):57-63.

383 Sun Xiangyang. A Study on Forest Soil CO<sub>2</sub>, N<sub>2</sub>O and CH<sub>4</sub> Emission Flux and Dynamics in Xishan  
384 Area, Beijing[D]. 1999.

385 Teepe R, Ludwig B. Variability of CO<sub>2</sub> and N<sub>2</sub>O emissions during freeze thaw cycles: Results of  
386 model experiments on undisturbed forest soil cores[J].Journal of Plant Nutrition and Soil  
387 Science. 2004,16(7):153-159.

388 Wang G, Du R, Kong Q, et al. Experimental study on soil respiration of temperate grassland in  
389 China[J]. Chinese Science Bulletin. 2004,49(6):642-646.

390 WMO Greenhouse Gas Bulletin (GHG Bulletin) - No. 15: The State of Greenhouse Gases in the  
391 Atmosphere Based on Global Observations through 2018, World Meteorological Organization  
392 (WMO), 2019.

393 WMO Greenhouse Gas Bulletin (GHG Bulletin) - No. 5: The State of Greenhouse Gases in the  
394 Atmosphere Using Global Observations through 2008, World Meteorological Organization  
395 (WMO), 2009.

396 ZHANG Lihua, SONG Changchun, WANG Dexuan. CO<sub>2</sub>, CH<sub>4</sub> and N<sub>2</sub>O emissions to the  
397 atmosphere upon nitrogen addition in the swamp wetland[J]. Acta Scientiae Circumstantiae.  
398 2005,25(8):1112-1118.

# Figures

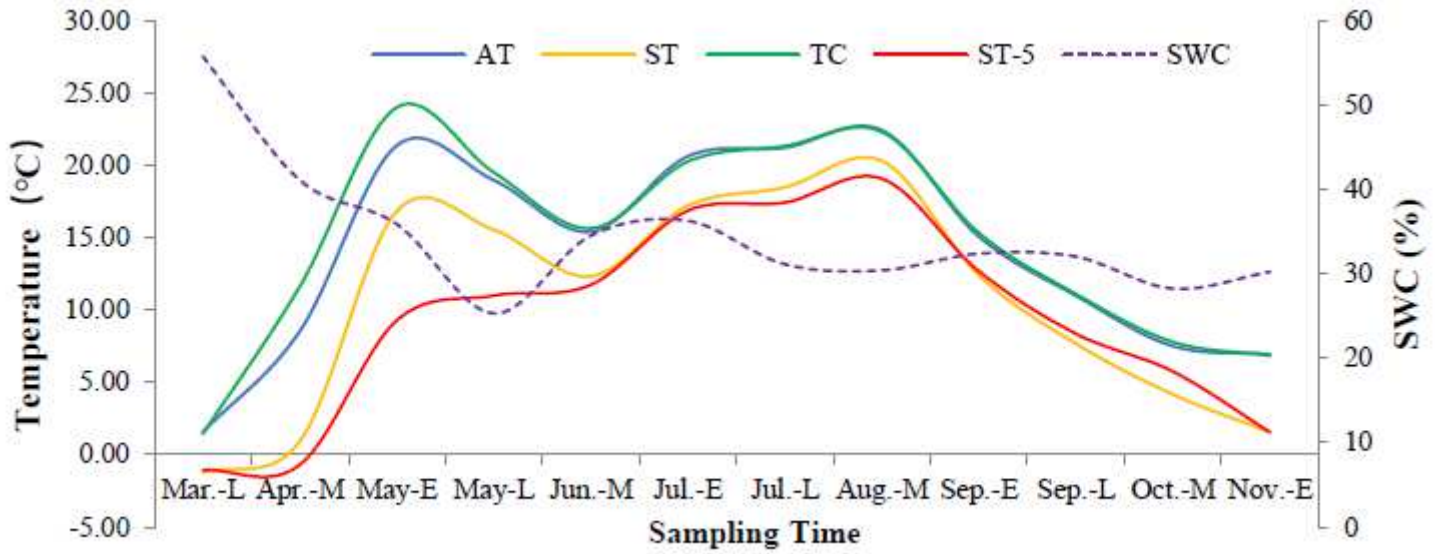


Figure 1

Variation process of the environmental factors in the year

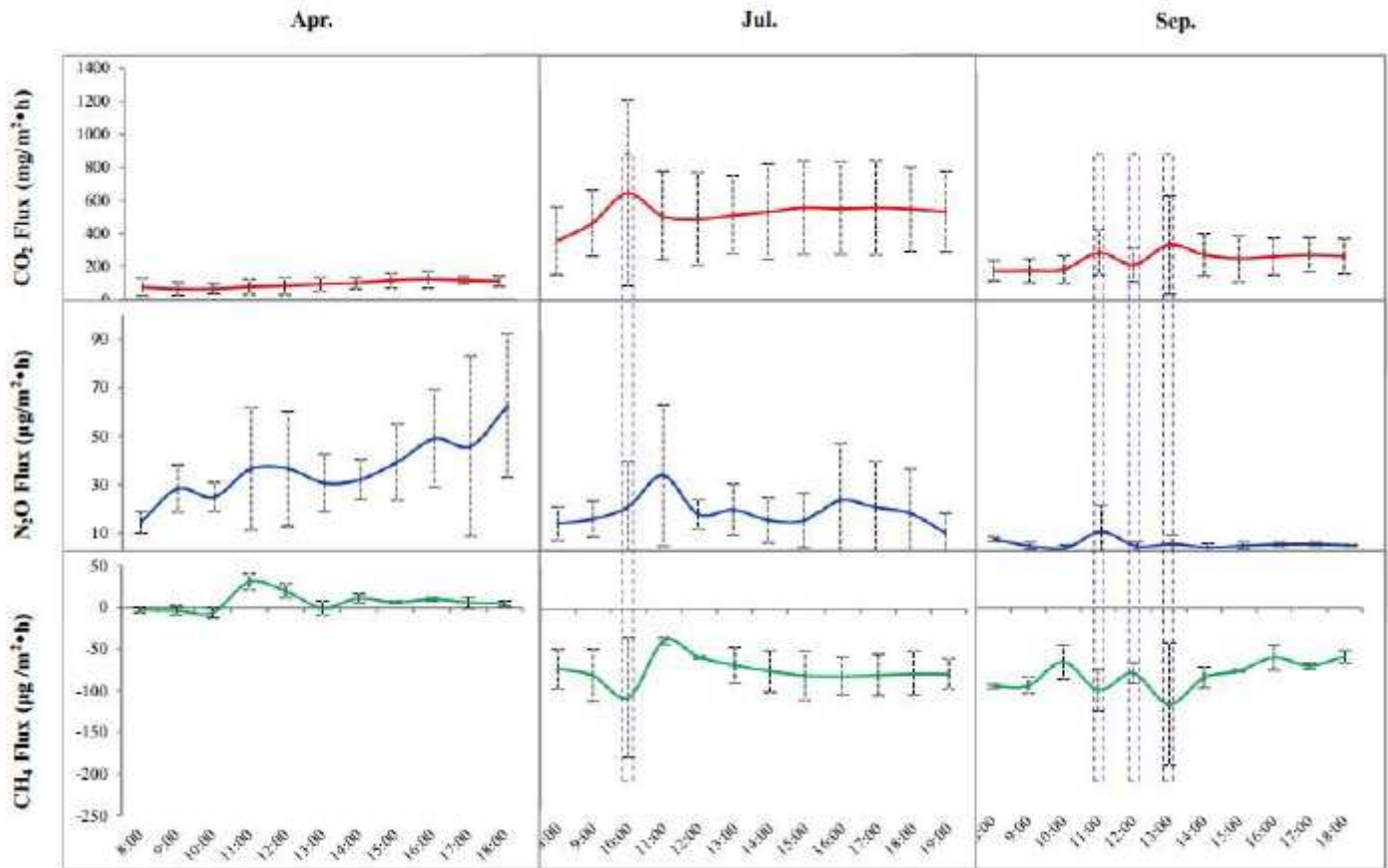


Figure 2

Dynamic process of GHGs flux rate during a day in different seasons

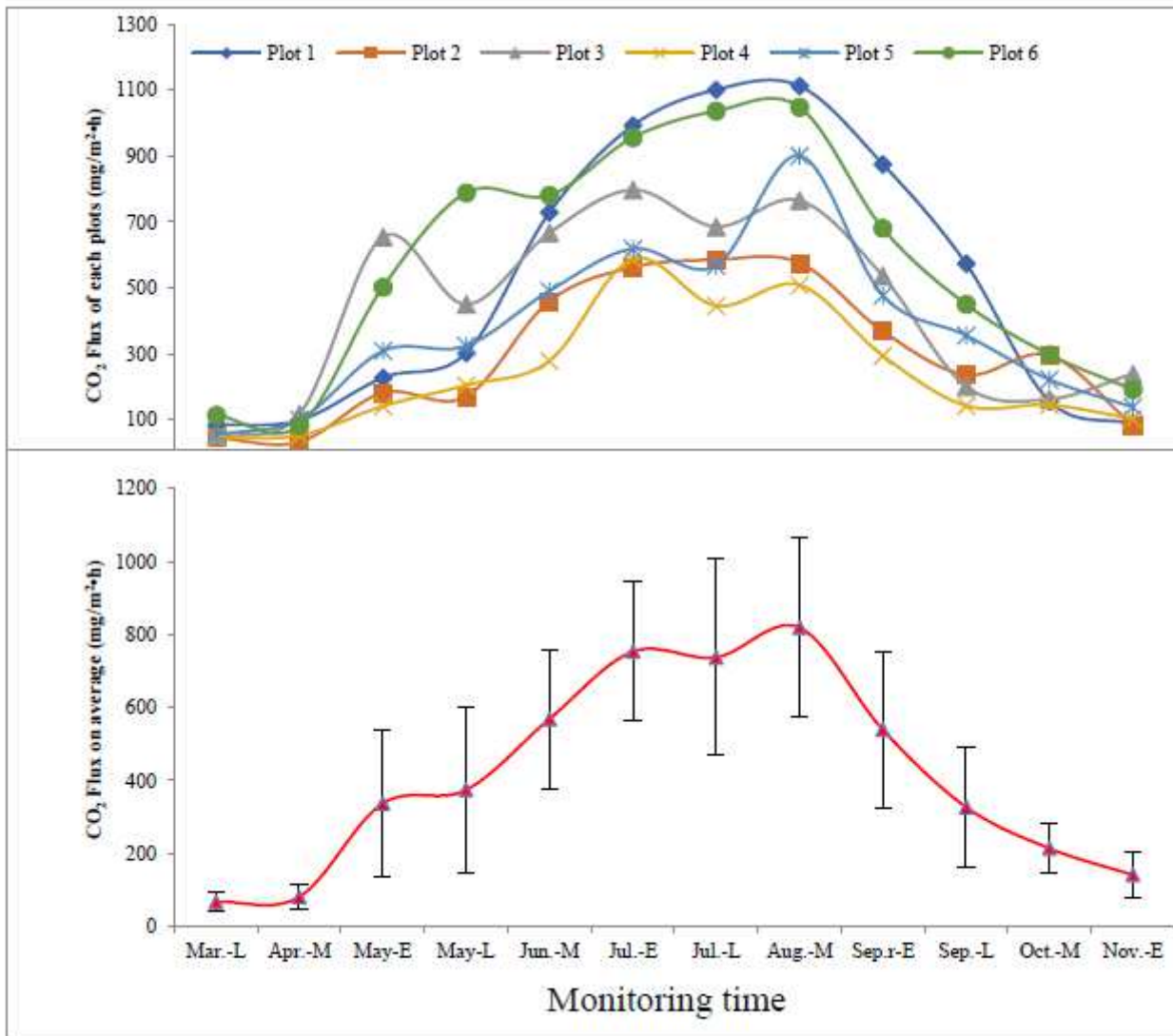
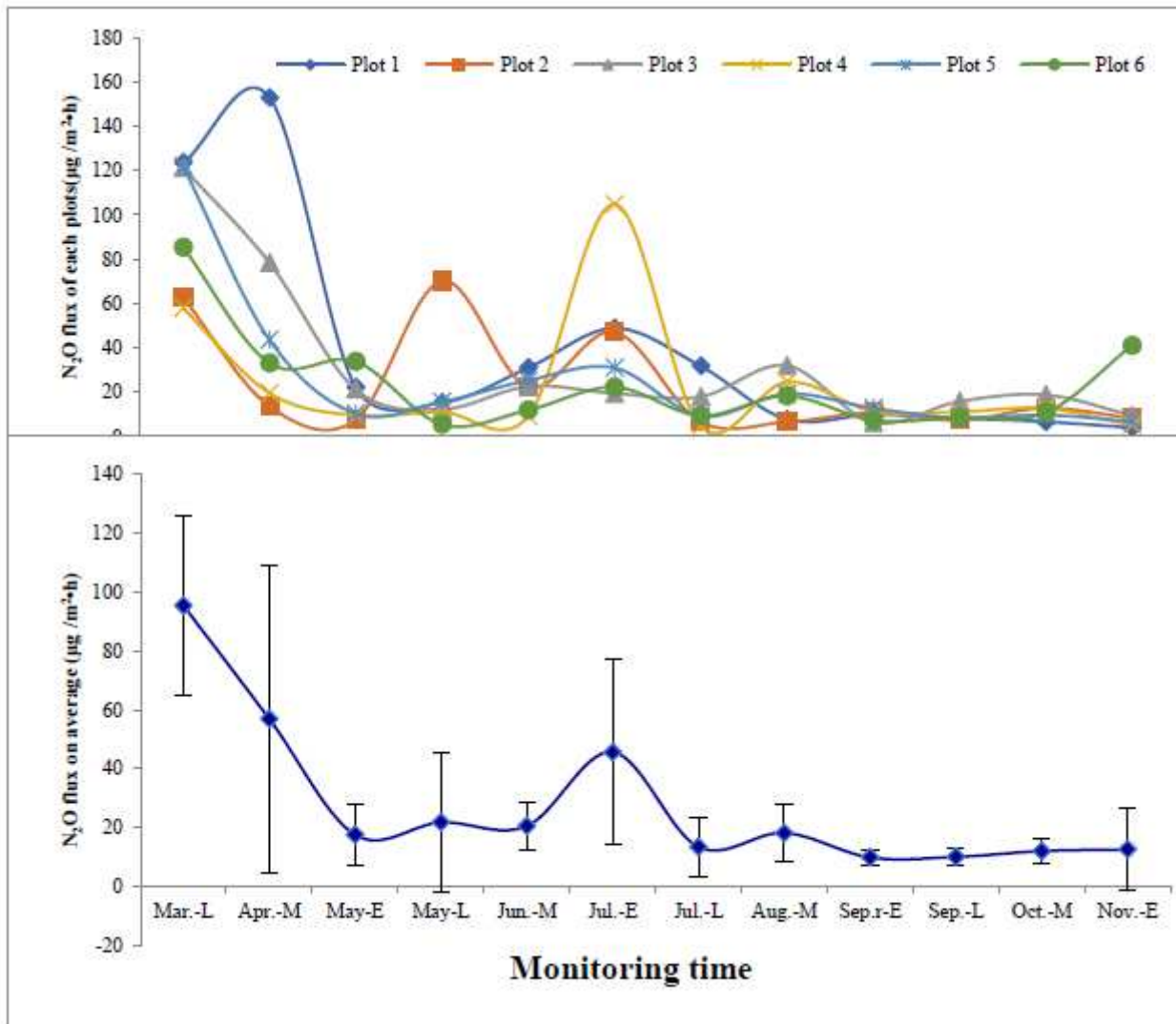


Figure 3

Dynamic process of CO<sub>2</sub> flux rate in different seasons



**Figure 4**

Dynamic process of N<sub>2</sub>O flux rate in different seasons

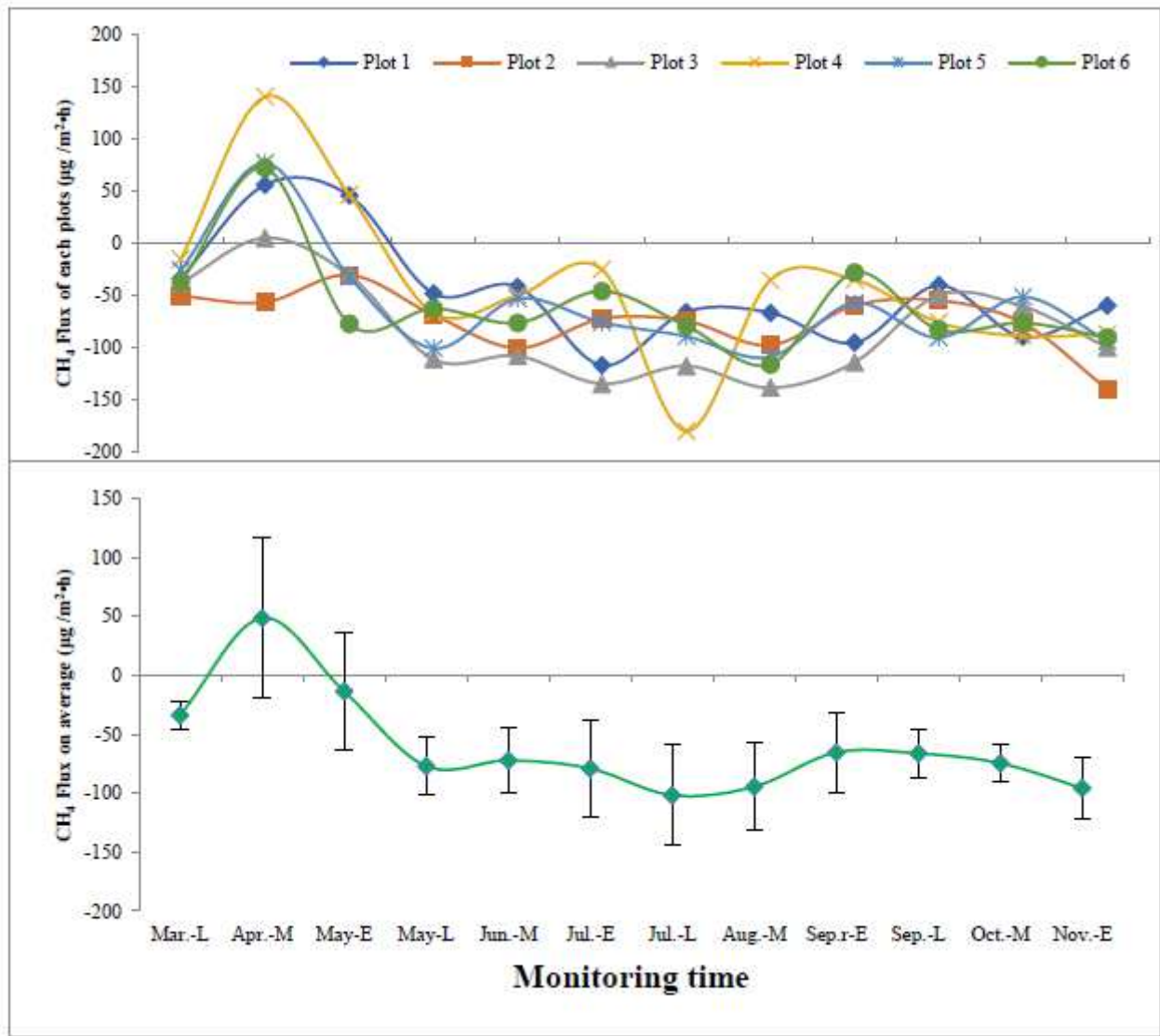


Figure 5

Dynamic process of CH<sub>4</sub> flux rate in different seasons